Dynamic Modeling and Control of a Parallel Upper-limb Rehabilitation Robot

Liang Peng, Zeng-Guang Hou, Weiqun Wang

***Abstract*—This paper aims at dynamic modeling and control of a new upper-limb rehabilitation robot which has a parallel structure. Dynamic modeling of parallel robot is a complicated problem, and the dynamics and voluntary force of the patient arm increase the difficulty of dynamic analysis and control in rehabilitation training. The novelties of this study are: (1) dynamics of the robot and the patient are considered together, and this human-robot interaction system is modeled as a redundantly actuated closed-chain system (2 DOFs, 4 active joints); (2) the system dynamics are derived in workspace using a new method based on the dynamics of its three serial open-chain branches, and both kinematic constrains and interaction forces are considered during the derivation. Compared with the other two previous methods reviewed in this paper, the proposed method is easier to derive, more computationally efficient, and it can be used in both redundant and non-redundant cases. Besides, a model based PD-computed torque controller is designed and the simulation of passive training task along a circular path is presented to prove the effectiveness of this method.**

I. Introduction

With the rapid growth of post-stroke population in the last two decades, many robotic systems have been developed to assist rehabilitation training of patients with motor disorders [1], [2]. On one hand, robots are more appropriate to do repetitive and labourious tasks, which can help alleviate the shortage of the physical therapists and reduce their physical burdens. Besides, widespread utilization of rehabilitation robots will help reduce treatment costs and guarantee training intensity and outcomes [3].

The main work of rehabilitation robot is to assist the patient to complete some movement tasks along desired trajectories, and passive training is one of the fundamental training modes, where 'passive' means that the patient is carried by the robot to move passively along predefined trajectories [4]. Passive training is a trajectory tracking problem for robot control, and the difficulty lies in the nonlinear characteristics of the robot. Moreover, for rehabilitation training applications, the inclusion of human limb and unexpected voluntary forces add more difficulty and uncertainty to the system.

In this paper, a novel upper limb rehabilitation robot is introduced, which has a 2-DOF parallel structure as shown in Fig. 1(a). Parallel design has many advantages over its serial counterparts such as high stiffness, simple joint design, low inertial etc [5]. As shown in Fig. 1(a), five links of the robot are connected by revolute joints to form a closed-chain mechanism, where only two joints at the base are active (actuated by DC motors via the cable transmission system), while the others are passive. As the motions of passive joints are dependent on active joints, it's difficult to perform kinematic and especially dynamic analysis [6].

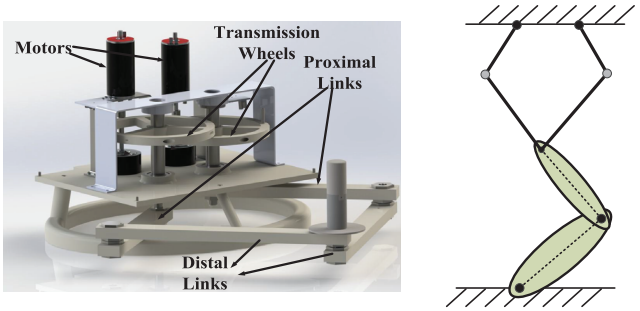

Fig. 1. (a) is the structure of the rehabilitation robot, and (b) is the diagram of upper limb training with the robot.

Besides the complexity of the parallel robot itself, the rehabilitation training task includes the other dynamic system - the patient's arm. As shown in Fig. 1(b), the human arm is coupled with the robot at the end-effector, which can moves in the horizontal plane. For simplicity of control, the human arm and muscle forces are ignored in previous studies [7], and regarded as modelling error and external disturbance, respectively. For system dynamic analysis and simulation purpose, however, the human arm dynamics and voluntary force should be included, as they are comparable with and have large influence on the rehabilitation robot dynamics.

In this paper, for dynamic analysis purpose, the human-robot system is regarded as a redundantly actuated closed-chain robot, which has two DOFs, and is driven by two DC motors and human muscles. The entire human-robot system dynamics is derived based on the dynamics of its three serial branches. As the kinematic constrains and interaction forces between these serial branches are easily represented in task space, this redundant closed-chain dynamic modeling problem is solved in task space rather than joint space as in conventional methods [6]. Compared with the other two previous methods [8], [9] reviewed in this paper (in Section II), this method is easy to understand and more computationally efficient, and the model based control algorithms can be

*This research is supported in part by the National Natural Science Foundation of China (Grants 61225017, 61175076, 61203342), and the International S&T Cooperation Project of China (Grant 2011DFG13390).

The authors are with The State Key Laboratory of Management and Control for Complex Systems, Institute of Automation, Chinese Academy of Sciences, Beijing 100190, China Emails:{liang.peng, zengguang.hou, weiqun.wang}@ia.ac.cn

978-1-4799-1808-9/15/$31.00 ©2015 IEEE

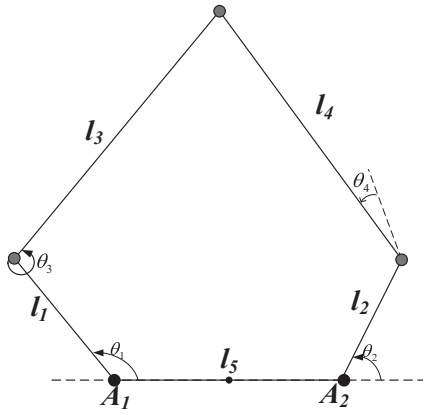

Fig. 2. Two-DOF parallel mechanism.

implemented easily [10].

II. Dynamic Modelling and Model Based Controller Design

A. Problem Setup

As shown in Fig. 1(b), the human upper limb is simplified and regarded as a 2-DOF serial robot, which is actuated by several groups of muscles. For simplicity, the trunk of the patient is assumed to be static, which is reasonable as the patient usually sits still on the chair during training, and his/her body moves little.

On the other hand, the robot is simplified as a five-bar parallel mechanism, and the position of the end-effector (the handle) coincide with that of the human hand. As a result, the entire human-robot system can be regarded as a combination of a serial robot and a parallel robot, which have kinematic constrains and interact at the end-effector.

As the human arm and the robot are coupled and interact at the end-effector, it's more appropriate to regard them as one human-robot system. This system can move in the plane so the DOF is 2, and the system is driven by two DC motors and two human joints, which means it has four actuators. Therefore, the human-robot system dynamic modeling problem can be transformed into a redundantly actuated closed-chain robot modelling problem.

B. Previous Methods Review

1) Reduced Model Method:

The main idea of this method is: first, Lagrangian method is applied directly on the close-chain robot assuming all joints are active joints, and a redundant dynamic model with respect to all joints is derived. Second, the kinematic constrains are added to the redundant dynamic model, and the reduced model which contains only independent variables is obtained [8].

An illustrative modeling example in [8] is shown in Fig.2, which has a similar structure to our robot, and the Lagrangian energy equation of the robot is:

$$E = \sum_{i=1}^{4} \frac{1}{2}[m_i(\dot{x}_{si} + \dot{y}_{si})^2 + I_i\dot{\theta}_i^2] + P \tag{1}$$

where m_i, I_i are the mass and inertial of four moving links, and (x_{si}, y_{si}) are the coordinates of the mass center of each moving links, and P is the potential energy of the entire system which doesn't change in our case as the robot moves in the horizontal plane.

Applying Lagrange method with respect to all joints:

$$\frac{d}{dt}\frac{\partial E}{\partial \dot{\theta}} - \frac{\partial E}{\partial \theta} = \tau$$

we can obtain the dynamics in the following form:

$$D'(q')\ddot{q}' + C'(q', \dot{q}')\dot{q}' = \tau' \tag{2}$$

where $q' = [\theta_1\ \theta_2\ \theta_3\ \theta_4]^T$

Therefore, (2) is the dynamics equation assuming all joints being active.

If we define

$$\begin{aligned} \dot{q}' &= \rho(q')\dot{q} \\ q' &= \sigma(q) \end{aligned} \tag{3}$$

where

$$q = [\theta_1\ \theta_2]^T$$

the reduced dynamics equation can be obtained:

$$D(q')\ddot{q} + C(q', \dot{q}')\dot{q} = \tau \tag{4}$$

where

$$\begin{aligned} &D(q') = \rho(q')^T D'(q')\rho(q') \\ &C(q', \dot{q}') = \rho(q')^T C'(q', \dot{q}')\rho(q') + \rho(q')^T D'(q')\dot{\rho}(q', \dot{q}') \end{aligned}$$

Remark: As the dynamics is established assuming all joints are active at first, the computation procedures as in (2) and (4) have many high-order (6×6 in our case) matrix operations; secondly, it's difficult to derive the joint angle relationship as in (3) for our case which has three kinematic constrains and four active joints for a 2-DOF robot.

2) Lagrange-D'Alembert Formulation Based Method:

The second method proposed in [9] builds the redundant closed-chain dynamics from simple serial nonredundant open-chain dynamics, and can be used for both closed-chain and redundant mechanisms. The illustrative example in [9] is shown in Fig. 3a, where the robot has 2 DOFs with 3 active joints (on the base) and 3 passive joints.

The modelling procedure can be summarized into 2 steps:

Step 1: The closed-chain robot is virtually cut to form an open-chain systems which are considered to be independent at first, as shown in Fig. 3b. Then the dynamics of the open-chain system can be obtained using Lagrangian method:

$$D(q)\ddot{q} + C(q, \dot{q})\dot{q} = \tau \tag{5}$$

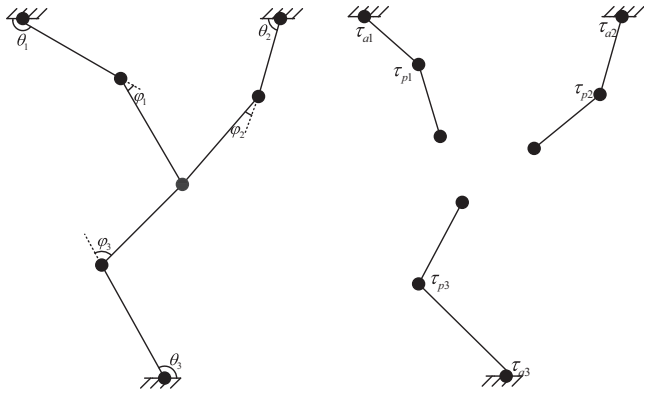

Fig. 3. Two-DOF redundant parallel mechanism and its equivalent open-chain system.

where

$$q = [\quad \theta_1 \quad \theta_2 \quad \theta_3 \quad \varphi_1 \quad \varphi_2 \quad \varphi_3 \quad]^T$$
$$\tau = [\quad \tau_{a1} \quad \tau_{a2} \quad \tau_{a3} \quad \tau_{p1} \quad \tau_{p2} \quad \tau_{p3} \quad]^T$$

Step 2: To produce the same movement, the torque inputs of closed-chain and open-chain have the following relationship:

$$W^T\tau = S^T\tau_a \tag{6}$$

where matrixes W and S are defined as:

$$W = \frac{\partial q}{\partial q_e} = \begin{bmatrix} \frac{\partial q_a}{\partial q_e} \\ \frac{\partial q_p}{\partial q_e} \end{bmatrix}$$
$$S = \frac{\partial q_a}{\partial q_e}$$

Equation (6) is proved based on Lagrange-D'Alembert Formulation, and the derivation details can be found in [9].

Substituting (6) into (5), we have

$$W^T(D(q)\ddot{q} + C(q,\dot{q})\dot{q}) = S^T\tau_a \tag{7}$$

where q_a represents the active joints and q_e represents the vector of independent generalized coordinates of the system, and in [9] they are defined as:

$$q_a = [\ \theta_1 \quad \theta_2 \quad \theta_3\ ]^T,\ q_e = [\ x \quad y\ ]^T$$

By making use of the kinematic constraints

$$\dot{q} = \frac{\partial q}{\partial q_e}\dot{q}_e = W\dot{q}_e$$
$$\ddot{q} = \dot{W}\dot{q}_e + W\ddot{q}_e$$

the dynamic equations of a redundant closed-chain mechanism is obtained:

$$\hat{D}\ddot{q}_e + \hat{C}\dot{q}_e + \hat{C} = S^T\tau_a \tag{8}$$

where

$$\hat{D} = W^T D W$$
$$\hat{C} = W^T D\dot{W} + W^T C\dot{W}$$

Remark: This method can be used in both parallel and redundant robot dynamic modelling, and theoretically q_e can be joint angles or end-effector coordinates. However, it's difficult to derive the matrix W if q_e is joint angle, so the example in [9] is developed in task space. Besides, as in the first method above, the derivation also contains many high order matrix operations.

C. Proposed Dynamic Modelling Method

In our method, the closed-chain robot is also regarded as three open-chain serial robots with kinematic constrains at the end-effector as in the second method above. However, both kinematic constrains and interaction forces are considered at the same time when we derive the dynamics equation of each serial open-chain branch.

For the first serial branch, it's easy to obtain its dynamics equation as:

$$D_1\ddot{q}_1 + C_1\dot{q}_1 = \tau_1 + J_1^T F_1 \tag{9}$$

where

$$q_1 = [\ \theta_1 \quad \varphi_1\ ]^T$$
$$\tau_1 = [\ \tau_{a1} \quad \tau_{p1}\ ]^T$$

and F_1 is the force at the end-effector imposed by the other two branches.

As joint P_1 is passive, we have $\tau_{a1} = 0$.

According to the definition of Jacobian equation:

$$\dot{X} = J_1\dot{q}_1$$

we have:

$$\begin{aligned} \dot{q}_1 &= J_1^{-1}\dot{X} \\ \ddot{q}_1 &= \dot{J}_1^{-1}\dot{X} + J_1^{-1}\ddot{X} \\ &= -J_1^{-1}\dot{J}_1 J_1^{-1}\dot{X} + J_1^{-1}\ddot{X} \end{aligned} \tag{10}$$

Then the dynamics equation can be transformed into:

$$\begin{aligned} &D_1(-J_1^{-1}\dot{J}_1 J_1^{-1}\dot{X} + J_1^{-1}\ddot{X}) + C_1 J_1^{-1}\dot{X} \\ &= {J_1}^T(J_1^{-T}\tau_1 + F_1) \Leftrightarrow \\ &J_1^{-T} D_1 J_1^{-1}\ddot{X} + J_1^{-T}(-D_1 J_1^{-1}\dot{J}_1 + C_1)J_1^{-1}\dot{X} \\ &= J_1^{-T}\tau_1 + F_1 \end{aligned} \tag{11}$$

If we define:

$$\hat{D}_1 = J_1^{-T} D_1 J_1^{-1}$$
$$\hat{C}_1 = J_1^{-T}(-D_1 J_1^{-1}\dot{J}_1 + C_1)J_1^{-1}$$

then the dynamics of the first serial branch is derived in workspace:

$$\hat{D}_1\ddot{X} + \hat{C}_1\dot{X} = J_1^{-T}\tau_1 + F_1 \tag{12}$$

In the same manner, the dynamics of the second serial branch of the robot can be derived as:

$$\hat{D}_2\ddot{X} + \hat{C}_2\dot{X} = J_2^{-T}\tau_2 + F_2 \tag{13}$$

where

$$\hat{D}_2 = J_2^{-T} D_2 J_2^{-1}$$
$$\hat{C}_2 = J_2^{-T}(-D_2 J_2^{-1}\dot{J}_2 + C_2)J_2^{-1}$$

and

$$\tau_2 = \begin{bmatrix} \tau_{a2} & 0 \end{bmatrix}^T$$

For the human limb branch, we have:

$$\hat{D}_3\ddot{X} + \hat{C}_3\dot{X} = J_3^{-T}\tau_3 + F_3 \tag{14}$$

where

$$\hat{D}_3 = J_3^{-T} D_3 J_3^{-1}$$
$$\hat{C}_3 = J_3^{-T}(-D_3 J_3^{-1}\dot{J}_3 + C_3)J_3^{-1}$$

and

$$\tau_3 = \begin{bmatrix} \tau_{a3} & \tau_{p3} \end{bmatrix}^T$$

It should be noted that, for the patient's arm, both shoulder and elbow joints have torque outputs, so $\tau_{p3} \neq 0$.

During the derivation above: (1) we have considered the kinematic constrains at the end-effector, which means the end-effector coordinates X in (12), (13), and (14) are the same; (2) the interaction forces between the end-effectors of three serial branches are included, which are F_1, F_2, and F_3, respectively; (3) both active and passive joints are considered in the derivation. Therefore, (12), (13), and (14) constitute the dynamics of this redundantly actuated closed-chain system.

By adding three dynamics equations (12), (13), and (14) together, we can obtain:

$$\begin{aligned} &\left(\hat{D}_1 + \hat{D}_2 + \hat{D}_3\right)\ddot{X} + \left(\hat{C}_1 + \hat{C}_2 + \hat{C}_3\right)\dot{X} \\ &= \left(J_1^{-T}\tau_1 + J_2^{-T}\tau_2 + J_3^{-T}\tau_3\right) + (F_1 + F_2 + F_3) \end{aligned}$$

For each serial branch, the force exerted by the other two branches and the force it imposed on other branches are acting force and reaction force, which are same in amplitude and opposite in direction, so we have

$$F_1 + F_2 + F_3 = 0$$

Therefore, the dynamic equation of the redundant closed-chain system is:

$$\begin{aligned} &\left(\hat{D}_1 + \hat{D}_2 + \hat{D}_3\right)\ddot{X} + \left(\hat{C}_1 + \hat{C}_2 + \hat{C}_3\right)\dot{X} \\ &= J_1^{-T}\tau_1 + J_2^{-T}\tau_2 + J_3^{-T}\tau_3 \end{aligned} \tag{15}$$

If we define:

$$\begin{aligned} &\hat{D} = \hat{D}_1 + \hat{D}_2 + \hat{D}_3 \\ &\hat{C} = \hat{C}_1 + \hat{C}_2 + \hat{C}_3 \\ &F = {J_1}^{-T}(\theta_1, \varphi_1)\tau_1 + {J_2}^{-T}(\theta_2, \varphi_2)\tau_2 + {J_3}^{-T}(\theta_3, \varphi_3)\tau_3 \end{aligned} \tag{16}$$

(15) can be transformed into:

$$\hat{D}\ddot{X} + \hat{C}\dot{X} = F \tag{17}$$

where $\hat{D}$ is the Cartesian inertia term, $\hat{C}$ is the Cartesian Coriolis/centrifugal term, and F is the equivalent force of the robot joint torques at the end-effector.

It's easy to prove that (8) is equivalent to (15) when joint P_3 is considered to be active. However, the derivation of (8) has many 6×6 matrix operations as that in (5), which is more computationally expensive than our method.

D. PD-Computed Torque Control

The equivalent force input of the robot at the end-effector is defined as:

$$\begin{aligned} F &= \hat{D}\left(\ddot{X}_d + K_p e + K_d\dot{e}\right) + \hat{C}\dot{X} \\ &= \left(\hat{D}\ddot{X}_d + \hat{C}\dot{X}\right) + \hat{D}\left(K_p e + K_d\dot{e}\right) \end{aligned} \tag{18}$$

where e is the control error defined as:

$$e = \ddot{X}_d - X$$

and K_p, K_d are symmetric proportional and derivative gain matrices.

Substituting (18) into (17), we can obtain:

$$\ddot{e} = -K_p e - K_d\dot{e} \tag{19}$$

which is a linear error system.

The force input of the human-robot system includes both robot joint torques and human voluntary forces as in (15). However, in practice, the human voluntary force in rehabilitation training is not controllable and hard to detect or estimate. So for control purpose, the human force can be regarded as a kind of external disturbance, which is restrained by the PD controller.

Therefore the robot joint torque inputs can be obtained as:

$$\tau = J_r^T(\theta_1, \theta_2)F \tag{20}$$

where $J_r(\theta_1, \theta_2)$ is the Jacobian matrix of the rehabilitation robot defined as:

$$J_r(\theta_1, \theta_2) = \begin{bmatrix} \frac{\partial x}{\partial \theta_1} & \frac{\partial x}{\partial \theta_2} \\ \frac{\partial y}{\partial \theta_1} & \frac{\partial y}{\partial \theta_2} \end{bmatrix} \tag{21}$$

III. Simulation and Results

1) Human-robot System Simulation: Fig. 4 shows the definition of dynamics parameters of the human-robot system for simulation, where the robot is composed of four links l_1 to l_4, and the human arm is represented by links l_5 and l_6.

The simulation parameters are shown in TABLE I, including $mass$, $center\ of\ mass$, $moment\ of\ inertia$, and $length$ of each link, and the length of A_1A_2 is 12 cm. The robot's dynamics parameters are the real design values of our robot based on CAD software (SolidWorks 2012), and the human arm dynamics parameters are estimated based on the anthropometric data of a person who is 180 cm tall and 70 Kg in weight [11].

For serial branch 1, intermediate matrices in (9) are:

$$J_1 = \begin{bmatrix} -l_1\sin\theta_1 - l_3\sin(\theta_1 + \theta_3) & -l_3\sin(\theta_1 + \theta_3) \\ l_1\cos\theta_1 + l_3\cos(\theta_1 + \theta_3) & l_3\cos(\theta_1 + \theta_3) \end{bmatrix}$$

$$D_1 = \begin{bmatrix} d_{11} & d_{12} \\ d_{21} & d_{22} \end{bmatrix}$$

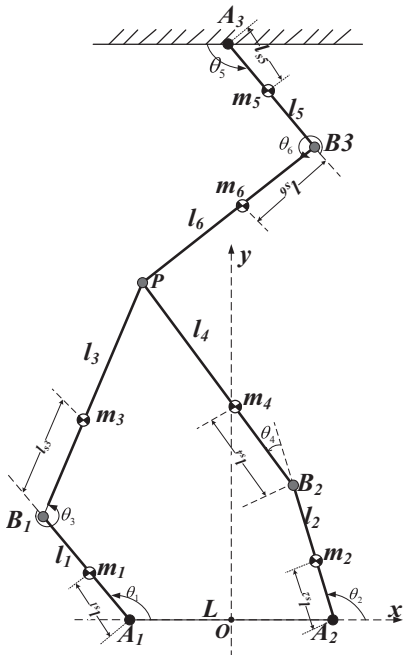

Fig. 4. Diagram of the human-robot system, and definition of the dynamics parameters.

Links	$l(m)$	$COM(m)$	$m(Kg)$	$I(kg.m^2)$
1	0.3	0.15	0.629	0.0047
2	0.3	0.15	0.629	0.0047
3	0.4	0.2	0.815	0.0109
4	0.4	0.2	0.815	0.0109
5	0.35	0.15	1.96	0.025
6	0.37	0.25	1.54	0.046

TABLE I. SIMULATION PARAMETERS

Of the parameters in the table, l is the length, COM is the distance between the center of mass and the proximal end, m is the mass, and I is the moment of inertia of the link about its center of mass.

where

$$d_{11} = m_1 l_{s1}^2 + m_3\left(l_1^2 + l_{s3}^2 + 2l_1 l_{s3}^2 + 2l_1 l_{s3}\cos\theta_3\right) + I_1 + I_3$$
$$d_{12} = d_{21} = m_3\left(l_{s3}^2 + l_1 l_{s3}\cos\theta_3\right) + I_3$$
$$d_{22} = m_3 l_{s3}^2 + I_3$$

$$C_1 = \begin{bmatrix} h\dot{\theta}_3 & h\dot{\theta}_3 + h\dot{\theta}_1 \\ -h\dot{\theta}_1 & 0 \end{bmatrix}$$

where

$$h = -m_3 l_1 l_{s3}\sin\theta_3$$

For the other two serial branches, the matrices have the similar form, except with their own dynamics parameters and joint angles.

2) Controller Simulation: The formation of PD-computed torque controller has been presented in the section above, and the torque inputs of the robot are:

$$\begin{aligned}\tau &= J_r^T(\theta_1,\theta_2)F \\ &= J_r^T\left(\left(\hat{D}_1+\hat{D}_2+\hat{D}_3\right)\left(\ddot{X}_d + K_p e + K_d\dot{e}\right)\right. \\ &\left.+\left(\hat{C}_1+\hat{C}_2+\hat{C}_3\right)\dot{X}\right)\end{aligned} \quad (22)$$

where the rehabilitation robot's Jacobian matrix J_r is:

$$J_r = B^{-1}A \quad (23)$$

where matrixes A and B are:

$$A = \begin{pmatrix} y\cos\theta_1 & 0 \\ -(x+\frac{L}{2})\sin\theta_1 & \\ 0 & y\cos\theta_2 \\ & +(\frac{L}{2}-x)\sin\theta_2 \end{pmatrix} l_1 \quad (24)$$

and

$$B = \begin{pmatrix} x+\frac{L}{2}-l_1\cos\theta_1 & y-l_1\sin\theta_1 \\ x-\frac{L}{2}-l_1\cos\theta_2 & y-l_1\sin\theta_2 \end{pmatrix} \quad (25)$$

3) Simulation Results: The simulation is coded in MATLAB (2012b, MathWorks, Natick, MA) environment, and the system states (acceleration, velocity, joint angles, end-effector position, etc.) are updated based on the human-robot dynamics (15) and robot torque inputs (22).

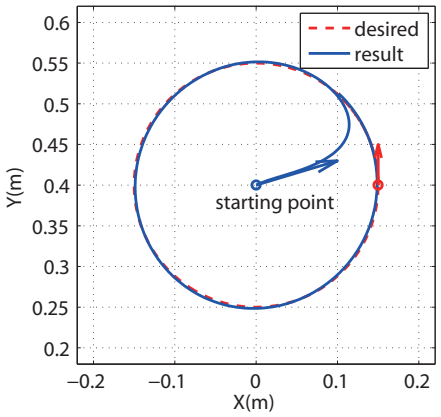

Fig. 5. Desired and actual trajectories of the circular path tracking task, where the robot and human hand start from the center of the circle.

In this simulation, the system dynamics are simulated by the fourth-order Runge-Kutta method (ode45 function in MATLAB), and the proportional matrix K_p and derivative matrix K_d of the controller (22) are selected as $\begin{bmatrix} 500 & 0 \\ 0 & 500 \end{bmatrix}$ and $\begin{bmatrix} 150 & 0 \\ 0 & 150 \end{bmatrix}$, respectively. The results of a circular passive training example are shown in Fig. 5, where the robot and the human hand start from the center of the circular path ((0, 0.4 m) in this simulation).

Therefore, the desired trajectories of the robot are:

$$\begin{cases} x_d(t) = R\cos\left(\frac{2\pi}{T_d}t\right) \\ y_d(t) = 0.4 + R\sin\left(\frac{2\pi}{T_d}t\right) \end{cases} \quad (26)$$

where $R = 0.15$ m is the radius, and $T_d = 8$ s is the period.

As we have mentioned before, the human voluntary force is hard to obtain in practice, so it's regarded as an external disturbance. In this simulation, the equivalent human voluntary force at the end-effector is set as:

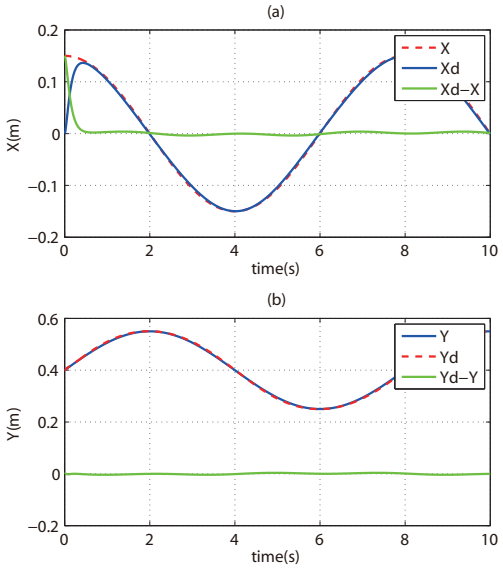

Fig. 6. Desired and actual trajectories, and tracking errors in X and Y directions.

$$\begin{cases} F_{hx} = A(t) \cdot \cos\left(\frac{2\pi}{T_d}t\right) \\ F_{hy} = A(t) \cdot \sin\left(\frac{2\pi}{T_d}t\right) \end{cases} \tag{27}$$

therefore we have:

$$F_h^T \dot{X}_d = 0$$

which means the human force is perpendicular to the velocity, and the amplitude is selected as:

$$A(t) = 5\sin\left(\frac{4\pi}{T_d}t\right) \tag{28}$$

so the human force works as a varying disturbance (maximum: 5 N, period: $\frac{T_d}{2} = 4$ s) perpendicular to the desired motion.

The desired and actual trajectories in X and Y directions are shown in Fig. 6, where the tracking errors are small ($\leq$1.2 mm), and smaller tracking errors can be obtained by adjusting the controller parameters K_p and K_d.

The robot torque inputs are shown in Fig. 7, where the maximum torques are set to be 5 N.m considering the saturation of motors in practice.

IV. Conclusion

This paper introduces a new upper-limb rehabilitation robot, which has a 2-DOF closed-chain structure, and proposes a new method to establish the human-robot interaction system dynamics. The human-robot system is modeled as a redundantly actuated closed-chain system (2 DOFs, 4 active joints), and the system dynamics are derived in workspace based on the dynamics of its three serial open-chain branches. Compared with the other two methods reviewed in this paper, the proposed method is easy to derive, and computationally efficient, and it can be used in both redundant and non-redundant cases. Besides, a PD-computed torque controller is designed and a simulation of circular path passive training task is given to prove the effectiveness of this method.

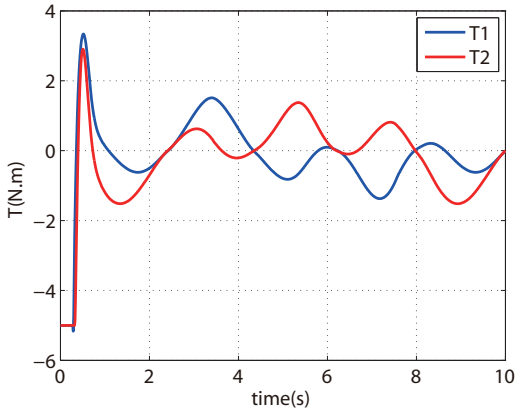

Fig. 7. Torque inputs of the robot based on PD-computed torque controller, and the maximum motor torque is 5 N.m in the simulation.

References

[1] A. S. Go, D. Mozaffarian, V. L. Roger *et al.*, "Heart disease and stroke statistics-2014 update: A report from the american heart association," *Circulation 2014*, pp. e28–e292, 2014.

[2] P. Maciejasz, J. Eschweiler, K. Gerlach-Hahn, A. Jansen-Troy, and S. Leonhardt, "A survey on robotic devices for upper limb rehabilitation," *Journal of NeuroEngineering and Rehabilitation*, vol. 11, no. 1, p. 3, 2014.

[3] V. Klamroth-Marganska, J. Blanco, K. Campen, A. Curt, V. Dietz, T. Ettlin, M. Felder, B. Fellinghauer, M. Guidali, A. Kollmar, A. Luft, T. Nef, C. Schuster-Amft, W. Stahel, and R. Riener, "Three-dimensional, task-specific robot therapy of the arm after stroke: a multicentre, parallel-group randomised trial," *The Lancet Neurology*, vol. 13, no. 2, pp. 159–166, 2014.

[4] L. Marchal-Crespo and D. Reinkensmeyer, "Review of control strategies for robotic movement training after neurologic injury," *Journal of NeuroEngineering and Rehabilitation*, vol. 6, no. 1, p. 20, 2009.

[5] G. Campion, W. Qi, and V. Hayward, "The pantograph mk-ii: a haptic instrument," in *Proceedings of IEEE/RSJ International Conference on Intelligent Robots and Systems (IROS)*, 2005, pp. 193–198.

[6] H. Yu, "Modeling and control of hybrid machine systems: a five-bar mechanism case," *International Journal of Automation and Computing*, vol. 3, no. 3, pp. 235–243, 2006.

[7] H. Jin, H. Zengguang, Z. Feng, C. Yixiong, and L. Pengfeng, "Training strategies for a lower limb rehabilitation robot based on impedance control," in *Proceedings of Annual International Conference of the IEEE Engineering in Medicine and Biology Society (EMBC)*, 2012, pp. 6032–6035.

[8] P. R. Ouyang, Q. Li, W. J. Zhang, and L. S. Guo, "Design, modeling and control of a hybrid machine system," *Mechatronics*, vol. 14, no. 10, pp. 1197–1217, 2004.

[9] C. Hui, Y. Yiu-Kuen, and L. Zexiang, "Dynamics and control of redundantly actuated parallel manipulators," *IEEE/ASME Transactions on Mechatronics*, vol. 8, no. 4, pp. 483–491, 2003.

[10] C. Long, L. Yingzi, H. Zeng-Guang, T. Min, H. Jian, and W. J. Zhang, "Adaptive tracking control of hybrid machines: A closed-chain five-bar mechanism case," *IEEE/ASME Transactions on Mechatronics*, vol. 16, no. 6, pp. 1155–1163, 2011.

[11] D. A. Winter, *Biomechanics and Motor Control of Human Movement*. John Wiley & Sons Ltd, UK, 2009.